

<b>Report Documentation Page</b>		<b>Form Approved OMB No.0704-0188</b>	
Public reporting for this collection of information is estimated 1 hour per response, including the time for reviewing instructions, searching existing data sources, gathering and maintaining the data needed and completing and reviewing the collection of information. Send comments regarding this burden estimate or any other aspect of this collection of information, including suggestions for reducing this burden, to Headquarters Services, Directorate for Information Operations and Reports, 1215 Jefferson Davis Highway, Suite 1204, Arlington, VA 22202-4302, and to the Office of Management and Budget, Paperwork Reduction Project (0704-0188), Washington, DC 20503.			
1. AGENCY USE ONLY (Leave blank)	2. REPORT DATE July 23, 1998	3. REPORT TYPE AND DATES COVERED Meeting Speech	
4. TITLE AND SUBTITLE Testing of Optical Materials for 193-nm Applications		5. FUNDING NUMBERS	
6. AUTHOR(S) V Liberman, M. Rothschild, J.H.C. Sedlacek, R.S. Uttaro, A. Grenville, A.K. Bates, C. Van Peski		C-F19628-95-C-0002 PE-	
7. PERFORMING ORGANIZATION NAME(S) AND ADDRESS(ES) Lincoln Laboratory, MIT 244 Wood Street Lexington, MA 02173-9108		8. PERFORMING ORGANIZATION REPORT NUMBER MS-12891	
9. SPONSORING/MONITORING AGENCY NAME(S) AND ADDRESS(ES)		10. SPONSORING/MONITORING AGENCY REPORT NUMBER ESC-TR-98-061	
11. SUPPLEMENTARY NOTES Volume 3427			
12a. DISTRIBUTION/AVAILABILITY STATEMENT Approved for Public Release; distribution is unlimited		12b. DISTRIBUTION CODE	
13. ABSTRACT (Maximum 200 words)			

We present an assessment of bulk fused silica and calcium fluoride, and of antireflective coatings for 193-nm lithographic applications. In the course of extensive marathon studies we have accumulated 1- 5 billion laser pulses on over 100 bulk material samples at fluences from 0.2 to 4 mJ/cm<sup>2</sup>/pulse. The results show large variation in both initial and induced absorption of fused silica (up to 40x for comparable irradiation doses ) and in densification of fused silica (almost an order of magnitude spread at the equivalent 10-year system lifetime). For antireflective coatings, there are samples that undergo no appreciable degradation when irradiated for >1 billion pulses at 15 mJ/cm<sup>2</sup>/pulse. However, initial losses in some coatings (up to 2%) may be unacceptably high for lithographic applications.

19990809 032

14. SUBJECT TERMS		15. NUMBER OF PAGES 8	
		16. PRICE CODE	
17. SECURITY CLASSIFICATION OF REPORT Unclassified	18. SECURITY CLASSIFICATION OF THIS PAGE Unclassified	19. SECURITY CLASSIFICATION OF ABSTRACT Unclassified	20. LIMITATION OF ABSTRACT Unclassified

**PROCEEDINGS OF SPIE REPRINT**



SPIE—The International Society for Optical Engineering

*Reprinted from*

***Optical Systems Contamination  
and Degradation***

20–23 July 1998  
San Diego, California



**Volume 3427**

# Testing of Optical Materials for 193-nm Applications

V. Liberman, M. Rothschild, J. H. C. Sedlacek, R. S. Uttaro

Lincoln Laboratory, Massachusetts Institute of Technology,  
244 Wood St., Lexington, MA 02420

A. Grenville

Intel Corporation, Hillsboro, OR 97124

A. K. Bates\*  
IBM/SEMATECH

C. Van Peski\*  
SEMATECH

## ABSTRACT

We present an assessment of bulk fused silica and calcium fluoride, and of antireflective coatings for 193-nm lithographic applications. In the course of extensive marathon studies we have accumulated 1- 5 billion laser pulses on over 100 bulk material samples at fluences from 0.2 to 4 mJ/cm<sup>2</sup>/pulse. The results show large variation in both initial and induced absorption of fused silica (up to 40x for comparable irradiation doses) and in densification of fused silica (almost an order of magnitude spread at the equivalent 10-year system lifetime). For antireflective coatings, there are samples that undergo no appreciable degradation when irradiated for >1 billion pulses at 15 mJ/cm<sup>2</sup>/pulse. However, initial losses in some coatings (up to 2%) may be unacceptably high for lithographic applications.

Keywords: 193-nm lithography, absorption, densification, laser-induced damage, antireflective coatings

## 1. INTRODUCTION

The relentless drive of the semiconductor industry to produce faster microprocessors and denser memory circuits has led to a continuous reduction in critical circuit dimensions. As the smallest circuit dimensions are pushed below 0.25  $\mu\text{m}$ , the lithographic tools required to print such small features are forced to employ shorter wavelength sources. In what may be one of the last generations of optical lithography, the tools are expected to handle the 193-nm excimer laser wavelength by the turn of the century.

Excimer laser lithography at the 193-nm wavelength places stringent demands on the required lifetime of optical components. The need to periodically replace the imaging optics would dramatically increase the cost of operating a lithography system. For this reason, if at all possible, the lens should have a lifetime no shorter than that of the tool – generally targeted at 10 years. Within this time frame, an element of a projection optics system will experience up to  $10^{11}$  pulses at laser repetition rates of 1 kHz and fluences per pulse ranging from 0.1 mJ/cm<sup>2</sup> to a few mJ/cm<sup>2</sup>.

The choice of optical materials that would meet both initial requirements of the 193-nm system and exhibit the required durability is limited. For instance, some materials with excellent transmission at 193-nm and good damage resistance, such as crystalline quartz and magnesium fluoride, are intrinsically birefringent, and are thus unsuitable for a lithographic system which is polarization-sensitive. Coupled with the initial requirements of low birefringence, candidate materials must exhibit excellent index homogeneity and must be available in sufficient quantity to meet the demand of the semiconductor manufacturing market.

The only practical materials that could meet the above requirements are crystalline calcium fluoride and amorphous fused silica. Even these materials become less transparent when exposed to billions of pulses of low-fluence 193-nm irradiation.

\* Mailing address: Lincoln Laboratory, Massachusetts Institute of Technology, Lexington, MA 02420

In addition to laser-induced transmission loss, amorphous materials such as fused silica undergo laser-induced densification or compaction. The main manifestations of compaction include physical shrinkage and a densification-induced increase of refractive index. Both these effects change the optical pathlength in an imaging system and thus adversely affect its performance. Historically, densification of glasses has been observed under irradiation by a variety of sources, dating back three decades: x-ray,<sup>1</sup> gamma-ray,<sup>2,3</sup> electron,<sup>3,4</sup> ion,<sup>5,6</sup> and neutron<sup>3</sup> irradiation. The studies observed a remarkable linearity on a log-log scale of measured densification,  $\delta$ , versus dose,  $D$ , over several decades of dose variation. Accordingly, the densification was fitted to the following formula:

$$\delta = k(D)^x, \quad (1)$$

where  $k$  and  $x$  are empirical constants with  $x < 1$ .

Recent studies have addressed 193-nm excimer-laser-induced densification of excimer-grade fused silica.<sup>7-9</sup> In this case, since the photon energy (6.4 eV) is less than the bandgap of fused silica ( $\approx 9$  eV for an upper valence band hole),  $D$  was identified as the number of two-photon absorption events. In general, the form of equation (1) was found to fit the results quite well, although a significant amount of scatter was reported in the data when  $\delta$  was plotted as a function of  $D$ . The  $x$ -parameter was found to lie in the range between 0.5 and 0.85, and the  $k$ -parameter was found to vary as well.

Optical coatings represent an integral part of a 193-nm exposure system since they are applied to virtually every surface, either for antireflective, reflective or beam splitting purposes. As with bulk materials, there are concerns about the durability and expected lifetime of these coatings in a production environment. Most studies of coatings damage addressed measurements of maximum energy required to produce damage to a coating in a single laser pulse.<sup>10,11</sup> Very few studies have dealt with durability of coatings over millions of pulses.<sup>12,13</sup>

We present interim results of a comprehensive study designed to assess the durability of candidate materials for lithographic applications at realistic irradiation conditions. Up to now we have exposed over 100 fused silica and CaF<sub>2</sub> bulk samples for  $>10^9$  pulses under fluences that would match those encountered in projection optics. We also present results of our assessment of antireflectance coatings from five major suppliers that have been exposed under marathon irradiation conditions.

## 2. BULK MATERIALS

### 2.1 Experimental

Our irradiation test bed (see Figure 1) uses 193-nm radiation from two free-running 400 Hz excimer lasers which are temporally interleaved for an effective 800 Hz pulse repetition rate. The incident laser beams are spatially overlapped by a 50/50 beam splitter, and subsequently distributed along 12 beamlines to deliver an incident laser fluence in the range 0.25 to  $>4$  mJ/cm<sup>2</sup>/pulse. At least 6 beamlines have a nominal fluence of 1 mJ/cm<sup>2</sup>/pulse. Each beam line passes through three sample stations for a total of 36 stations. At the beginning of each beamline we select the most uniform part of the laser beam with a 5-mm diameter aperture.

The fluence of each laser in front of every sample station is monitored *in situ* with three pyroelectric energy meters, travelling on three separate linear motor tracks that span the full width of the irradiation chamber. A reference power meter is used for measuring long-term drifts and for calibrating the energy meter readings. Every two million pulses we measure the energy from each laser in front of every station and the pulse duration of each laser. In addition the beam profile is checked periodically with a pyroelectric camera. The apertured beam is found to be essentially flat top (to within  $\pm 10\%$ ).

The whole irradiation setup is continuously nitrogen-purged to eliminate trace amounts of oxygen that could contribute to ozone formation from decomposition by 193-nm laser light. High ozone concentration inside the chamber would be undesirable, as it causes attenuation of 193-nm light. The ozone concentration in the box is constantly monitored and never exceeds 15 ppb.

All samples tested in this study are designated by the suppliers as "lithographic-grade" material. Some material is experimental, while other comes from production boules. Samples are provided unpolished with nominal dimensions of either 80 x 40 x 20 mm<sup>3</sup> or 40 x 25 x 25 mm<sup>3</sup>, and are then polished by a third party in order to standardize surface finish conditions. Unless otherwise noted, all the samples are irradiated and measured along their longest axis, i. e., 80 or 40 mm, respectively.

While assessment of in-situ beamline energies does allow us to obtain sample transmission at each station, in order to achieve better precision we periodically measure the transmission of all samples off-line with a laser ratiometric system. The setup employs a 45° incidence 50/50 beam splitter that divides a 193-nm laser beam into a probe and a reference beam. Each beam is incident onto a stationary energy meter. The sample being measured is placed into a fixture mounted on a linear track motor that can slide in and out of the probe beam to obtain a sample and a reference reading, respectively. For each individual measurement, we ratio the reading from the two detectors. Typically, one second each is allowed for a

sample and a reference reading. Depending on the laser repetition rate, 10-200 transmission readings are thus averaged, resulting in a measurement precision of 0.1 %, one standard deviation.

From the transmission data we extract an attenuation coefficient per cm, after correcting for Fresnel losses, and assuming multiple reflections inside the sample. All the attenuation and absorption coefficients reported here are base 10. For a sample of length  $l$  the internal transmission is:

$$T_{int} = 10^{-l(2\beta + (\alpha + \gamma)l)} \quad (2)$$

where  $\beta$  refers to a single surface loss, including both absorption and scatter,  $\alpha$  is the internal absorption coefficient per cm and  $\gamma$  is the bulk scatter coefficient per cm.

Surface losses are determined by performing three-axis laser transmission measurements along the 2-, 4-, and 8-cm directions, respectively. From these measurements we derive the value of  $\beta = 0.0015/\text{surface}$  for either fused silica or calcium fluoride, independent of grade. The magnitude of surface loss depends on the polishing conditions, and is not intrinsic to the material. In our experiments it is only a parameter used to correct the measured  $T_{int}$ . We note also that prior to performing the three-axis measurements, samples are irradiated in the nitrogen-purged measurement setup for  $\approx 10^5$  pulses in order to remove airborne adsorbates.

The value of  $\gamma$  at 193 nm is obtained by extrapolation of its experimentally measured values at 325, 442 and 633 nm.<sup>14</sup> Assuming a Rayleigh scattering dependence ( $\propto n^8/\lambda^4$ ), we obtain  $\gamma = 0.0008 \text{ cm}^{-1}$  for fused silica and  $<0.0001 \text{ cm}^{-1}$  for calcium fluoride, independent of material grade.

## 2.2 Densification measurements

We extract the densification of the samples from measurements of stress-induced birefringence at 633 nm. In general, the densification is a function of irradiation geometry, such as the fraction of the sample being irradiated. In order to apply the information obtained from a specific experiment to other geometries, we compute the unconstrained densification.<sup>8</sup> This is the densification that would occur if the whole sample were irradiated and allowed to compact freely. It is a geometry-independent quantity that is a function of only the material properties and the irradiation conditions.

The birefringence at 633 nm is measured off-line using two crossed polarizers and a photodiode detector. This system enables the determination of the unconstrained densification at a precision significantly better than 0.1 parts per million (ppm) at levels above 1 ppm. However, for low densification values the measurement is impacted by the initial stress distribution in the unirradiated sample. Our application of the birefringence measurement technique does not permit subtraction of the initial stress from the laser-induced stress, since only the magnitude but not the sign of stress can be obtained from birefringence measurements. For the purpose of this study, densification values of  $<1$  ppm are shown only for samples with sufficiently low initial birefringence ( $\leq 0.20 \text{ nm/cm}$ ).

## 2.3 Results

### 2.3.1 Initial and laser-induced absorption

Figure 2 shows representative absorption trends of fused silica and calcium fluoride as a function of pulse count. During the first 100 million pulses  $\alpha$  often appears to decrease for both fused silica and calcium fluoride (Figure 2A). This phenomenon may be attributed to a slow laser induced surface cleaning, or to partial bleaching of the bulk material. The lowest value of  $\alpha$  may be less than one fifth of its value as measured in the first few pulses (see top trace Figure 2A). After the initial decrease, the induced absorption may either level off (Figure 2A, top and bottom traces) or continue to grow steadily, sometimes at a very slow rate (Figure 2A middle trace). A different feature of the absorption shown in Figure 2B is the saturation of  $\alpha$  in some materials. Note that in this case, the saturation level ( $0.017 \text{ cm}^{-1}$ ) is too high for the material to be useful for lithographic applications (see discussion below). Finally, under our conditions there is no evidence of sudden absorption transition (SAT)<sup>15</sup> to at least 5 billion pulses.

Figure 3 shows the initial and added absorption of samples that have been exposed to a nominal fluence of  $1 \text{ mJ/cm}^2/\text{pulse}$ . Twenty  $\text{SiO}_2$  and  $\text{CaF}_2$  samples were selected for this figure from over 100 samples exposed under marathon irradiation conditions. The initial absorption values plotted here are the lowest  $\alpha$ , which occur sometimes at the start of irradiation and sometimes up to  $\sim 100$  million pulses later (see Figure 2). Several trends emerge from an analysis of Figure 3:

1. Many of the fused silica samples exhibit total  $\alpha$  (initial plus added) in excess of  $0.002 \text{ cm}^{-1}$  by the time their irradiation is completed. For a projection optics system comprised of a half meter of glass, this value of  $\alpha$  would result in a 20 % transmission loss. This relatively high level of  $\alpha$  is primarily caused by a combination of the short-wavelength tail of the  $\sim 220\text{-nm}$  E' color center and the long-wavelength tail of color centers below 190 nm. By contrast, high purity calcium fluoride appears to have an inherently higher damage resistance than fused silica (see also Ref. 12). The degradation in transmission of  $\text{CaF}_2$  is primarily caused by impurities, since there are no intrinsic color centers in the vicinity of 193 nm.

2. Significant variation in performance exists for both fused silica and calcium fluoride materials. For instance, for different grades of fused silica, induced absorption after similar irradiation dose can differ by up to 40 x (cf. Samples A and A' in Figure 3). The cause of such variation may be related to pre-existing defects, annealing history, OH content, H<sub>2</sub> content, or other parameters.

3. There does not appear to be a correlation between initial absorption and added absorption, especially for fused silica. For instance, the added absorption of sample B of Figure 3 is comparable to that of sample B'; however, the initial absorption of sample B is 40 times lower. This observation suggests that material selection on the basis of initial transmission measurements might be difficult. Rather, a good statistical database must be available for each grade of material considered. From the fundamental science point of view, this result supports the model that different phenomena are responsible for the initial (one-photon) absorption versus induced (multiphoton) color-center formation in fused silica.

### 2.3.2 Densification

Figure 4 presents a summary of unconstrained densification measurements plotted as a function of  $D$  for all the samples exposed in the fluence range of 0.25 to  $>4$  mJ/cm<sup>2</sup>/pulse. The dashed vertical line indicates an equivalent 10-year lifetime dose at a fluence of 0.1 mJ/cm<sup>2</sup>/pulse. The plot includes the data from over 20 samples, presented on a single chart to verify the applicability of a universal scaling law for all the materials. There is a considerable variation in densification across samples, resulting in almost an order of magnitude difference for the lifetime dose of 25 Mp·mJ<sup>2</sup>/cm<sup>4</sup>/ns. There does not appear to be a scaling law with unique coefficients  $k$  and  $x$  that could describe all samples. However, the seemingly quasi-random data points in Figure 4 are in fact comprised of individual strands belonging to data from separate samples obeying Equation (1), each with its own  $k$  and  $x$ . For illustrative purposes Figure 4 shows two such strands of data, belonging to two separate samples:  $k = 0.46$ ,  $x = 0.43$  for sample 1, and  $k = 0.34$ ,  $x = 0.55$  for sample 2. The variations of densification rates shown on Figure 4 can be attributed to differences among samples, among grades, or experimental conditions. More data are needed to verify the inter-batch and intra-batch consistency for given grades.

## 3. OPTICAL COATINGS

In an earlier work we have described preliminary results from our assessment of one-sided antireflective coatings under marathon irradiation conditions ( $>10^9$  pulses).<sup>16</sup> We have now completed an evaluation of two-sided antireflectance coatings from five different manufacturers. The coatings were exposed at fluences of 13-15 mJ/cm<sup>2</sup>/pulse for 1 to 1.2 billion pulses. Every 200 million pulses the transmittance and reflectance of the coatings is measured ex-situ, using a 12-degree spectrophotometer reflectance attachment. Before beginning marathon exposures, coatings were exposed in a ratiometric measurement setup (see above) to monitor effects of laser cleaning. The results of our findings can be summarized as follows.

1. Laser cleaning of coatings was found to vary in magnitude, depending on the sample, from  $<0.5\%$  to  $\approx 1.5\%$ . The main manifestation of the cleaning is transmission recovery with very small reflectance changes. The time scale for laser cleaning could be as short as  $10^4$  pulses or as long as  $10^6$  pulses at fluences of 10 mJ/cm<sup>2</sup>/pulse. Longer cleaning times were observed at lower fluences.

2. Initial losses in the antireflective coatings after laser cleaning (defined as  $100\% - \text{Reflectance} - \text{Transmittance}$ ) varied from  $<0.4\%$  to almost 2%. Initial losses did not affect subsequent coating durability. While specific optical designs of lithographic systems may place different constraints on the maximum allowable losses per coating, values of 2% loss are probably unacceptably high.

3. Several antireflectance coatings reached  $10^9$  pulses with minimum detectable degradation. In some cases, for coatings deposited on CaF<sub>2</sub> substrates, losses appeared to decrease for up to 1 billion pulses. The amount of this decrease (0.5 - 1%) is substantially higher than that expected from extrapolation of bleaching of bulk CaF<sub>2</sub> (see Figure 2 A, bottom trace). Therefore, such a decrease in loss must be a surface phenomenon.

## ACKNOWLEDGMENTS

The Lincoln Laboratory portion of this work was performed under a Cooperative Research and Development Agreement with SEMATECH. Opinions, interpretations, conclusions, and recommendations are those of the authors and are not necessarily endorsed by the United States Government.

## REFERENCES

- 1 W. Primak, "The X-ray compaction of vitreous silica," *Radiation Effects* **45**, 29-32 (1979).
- 2 J. A. Ruller and E. J. Friebele, "The effect of gamma-irradiation on the density of various types of silica," *J. Non-Cryst. Solids* **136**, 163-172 (1991).
- 3 W. Primak and R. Kampwirth, "The radiation compaction of vitreous silica," *J. Appl. Phys.* **39**, 5651-5658 (1968).
- 4 T. A. Deltin, D. A. Tichenor, and E. H. Barsis, "Volume, index-of-refraction, and stress changes in electron-irradiated vitreous silica," *J. Appl. Phys.* **48**, 1131-1138 (1977).
- 5 E. P. EerNisse, "Compaction of ion-implanted fused silica," *J. Appl. Phys.* **45**, 167-174 (1974).
- 6 W. Primak, "Mechanism for the radiation compaction of vitreous silica," *J. Appl. Phys.* **43**, 2745-2754 (1972).
- 7 T. P. Seward, III, C. Smith, N. F. Borrelli, and D. C. Allan, "Densification of synthetic fused silica under ultraviolet irradiation," *J. Non-Cryst. Solids* **222**, 407-414 (1997).
- 8 N. F. Borrelli, C. Smith, D. C. Allan, and T. P. S. III, "Densification of fused silica under 193 nm excitation," *J. Opt. Soc. Am. B* **14**, 1606-1615 (1996).
- 9 R. E. Schenker and W. G. Oldham, "Ultraviolet-induced densification in fused silica," *J. Appl. Phys.* **82**, 1065-1071 (1997).
- 10 E. Welsch, K. Etrich, H. Blaschke, P. Thomsen-Schmidt, D. Schafer, and N. Kaiser, "Investigation of the absorption induced damage in ultraviolet dielectric thin films," *Opt. Eng.* **36**, 504-514 (1997).
- 11 F. Rainer, W. H. Lowdermilk, D. Milam, C. K. Carniglia, T. T. Hart, and T. L. Lichtenstein, "Materials for optical coatings in the ultraviolet," *Appl. Opt.* **24**, 496-500 (1985).
- 12 D. J. Krajnovich, M. Kulkarni, W. Leung, A. C. Tam, A. Spool, and B. York, "Testing of the durability of single-crystal calcium fluoride with and without antireflection coatings for use with high-power KrF excimer lasers," *Appl. Opt.* **31**, 6062-6075 (1992).
- 13 J. Heber, R. Thielsch, H. Blaschke, N. Kaiser, K. Mann, E. Eva, U. Leinhos, and A. Gortler, "Stability of optical interference coatings exposed to low-fluence 193 nm ArF radiation," *Proc. SPIE* **3334**, 1041-1047 (1998).
- 14 T. Germer, unpublished work (1996).
- 15 D. J. Krajnovich, I. K. Pour, A. C. Tam, W. P. Leung, and M. V. Kulkarni, "Sudden onset of strong absorption followed by forced recovery in KrF laser-irradiated fused silica," *Opt. Lett.* **18**, 453-455 (1993).
- 16 V. Liberman, M. Rothschild, J. H. C. Sedlacek, R. S. Uttaro, A. Grenville, A. K. Bates, and C. V. Peski, "Assessment of optical coatings for 193-nm lithography," *Proc. SPIE* **3334**, 470-479 (1998).

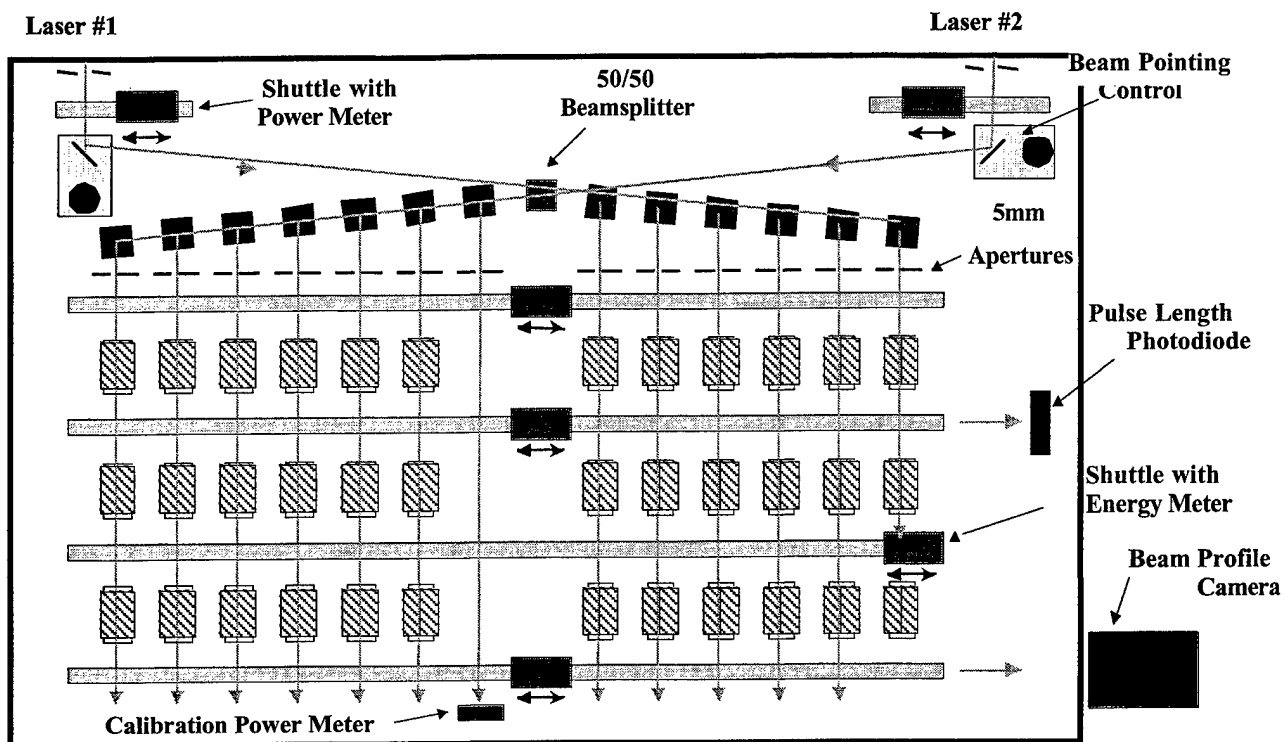


Figure 1. Experimental layout of the bulk marathon irradiation setup.

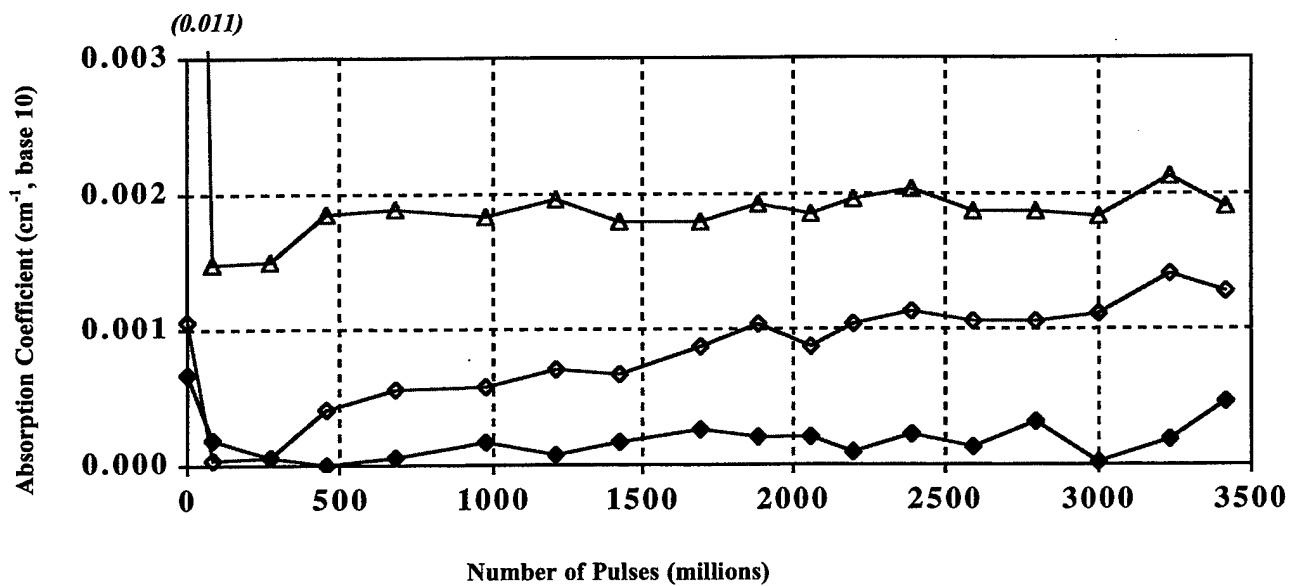


Figure 2A. Absorption coefficient of two fused silica samples (top and middle trace) and a calcium fluoride sample (bottom trace) as a function of number of pulses. The fluence is  $1 \text{ mJ/cm}^2/\text{pulse}$ .



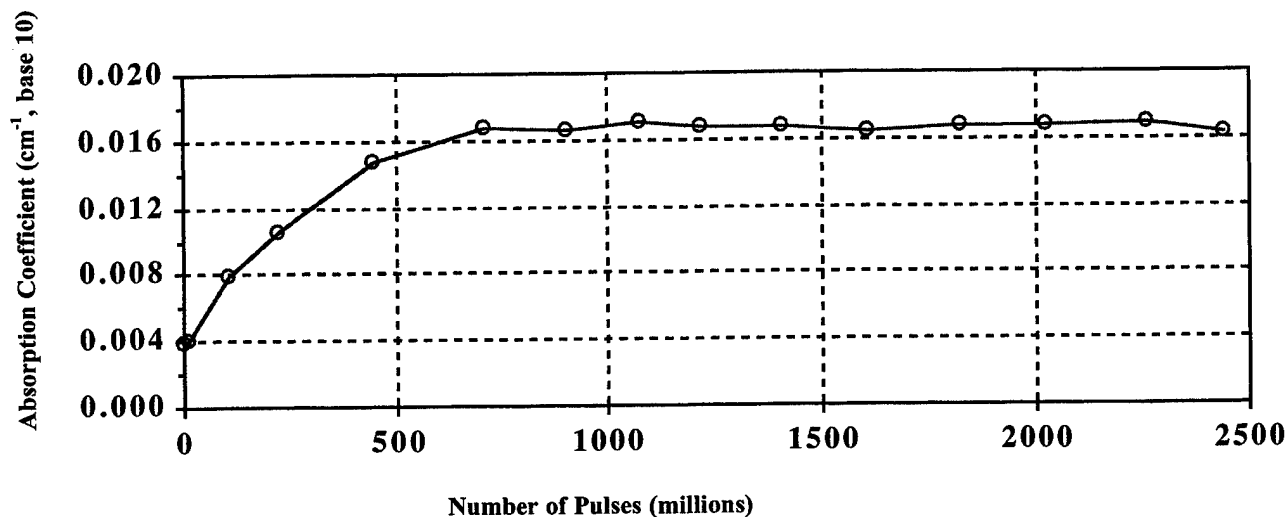


Figure 2 B. Absorption coefficient of a fused silica sample, showing saturation of absorption with exposure in millions of laser pulses. The fluence is 1 mJ/cm<sup>2</sup>/pulse.

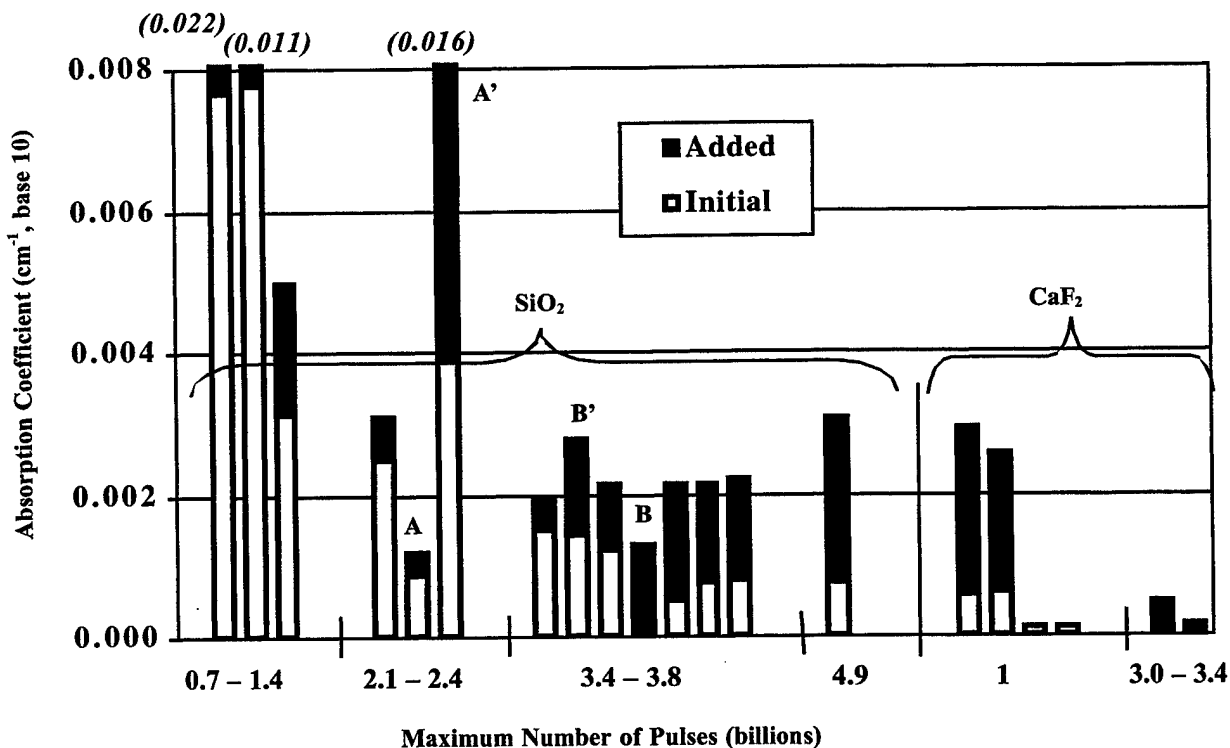


Figure 3. Initial and added absorption coefficients of 14 fused silica and 6 calcium fluoride representative samples. The numbers on the x-axis refer to the maximum number of pulses (in billions) that the samples have experienced. Nominal fluence is 1 mJ/cm<sup>2</sup>/pulse. See text for more details.

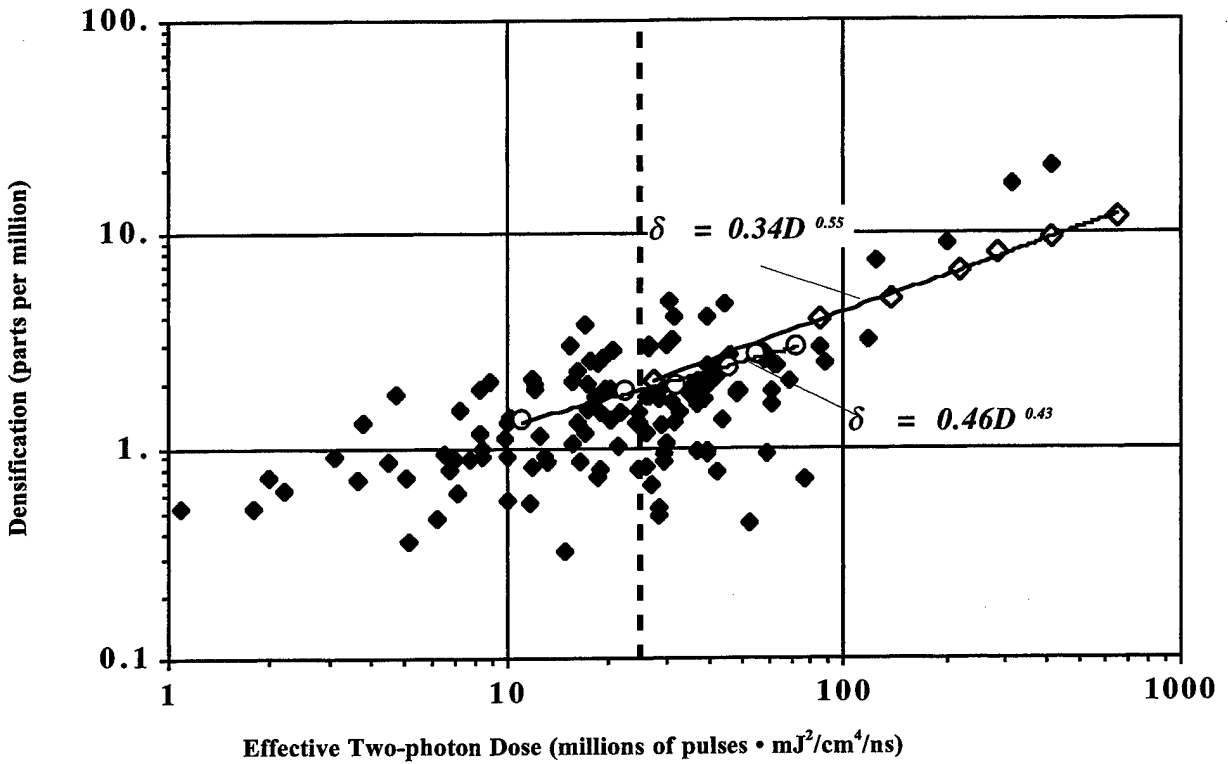


Figure 4. Laser-induced densification as a function of two-photon dose for SiO<sub>2</sub> samples. The units of dose are (millions of pulses · mJ<sup>2</sup>/cm<sup>4</sup>/ns). The vertical dashed line refers to an approximate lifetime dose of 25, corresponding to ten years of full-time operation at 0.1 mJ/cm<sup>2</sup>/pulse. Also shown are two series of data points corresponding to two separate samples and the least squares fit results to the equation (1). (See text for details.)